The titanium(IV) salt of *N*,*N*-(diphosphonomethyl)glycine: synthesis, characterisation, porosity and proton conduction

Enrique Jaimez, Gary B. Hix and Robert C. T. Slade*

Department of Chemistry, University of Exeter, Exeter, UK EX4 4QD

A new diphosphonic acid, *N*,*N*-(diphosphonomethyl)glycine, has been prepared. The titanium(IV) salt [Ti(dpmg)] of this acid has been characterised by X-ray powder diffraction, thermogravimetry, ^{31}P MAS NMR spectroscopy, isothermal N_2 adsorption–desorption and ac conductivity measurements. Phosphorus is present in a mixture of bonded phosphonate and free phosphonic acid groups. The material is both amorphous and porous (BET specific surface area = 119 m^2 g^{-1}), and its water content is relative humidity (RH)-dependent. Ti(dpmg) is a protonic conductor (at 90% RH and 90 °C, $\sigma = 3 \times 10^{-2}$ S cm^{-1}), with conductivity exhibiting Arrhenius-type behaviour at constant RH. Conductivity and Arrhenius parameters are strongly dependent on the water content.

Several recent studies have focused on the synthesis and crystal structure determination of layered phosphonates of di-, tri- and tetra-valent metals, *e.g.* ref. 1–3. In the case of tetravalent metals, the phosphonates usually have a layered structure, similar to that of their purely inorganic analogue α-zirconium phosphate $[Zr(HPO_4)_2 \cdot H_2O]$,[4] but with pendant organic groups (R) replacing the -OH groups in the interlayer region. Such solids can be synthesised with a wide range of R,[5] and combinations of two or more phosphonic acids may also be used.[6–8] These synthetic aspects can be exploited in designing new materials with potential applications such as sorption, ion exchange, chromatography, chiral molecular recognition, photochemistry, catalysis and ionic conduction,[9–15] and the reactivities of the pendant organic functions have also been studied.[1,16–19] In a recent review Kreuer highlighted the proton conductivities of layered acidic phosphates and phosphonates of zirconium(IV) in their hydrated and dry forms.[20] Layered phosphonates containing sulfonic acid groups in the organic moiety have conductivities approaching that of the sulfonated fluorocarbon polymer Nafion,[21,22] which is the electrolyte membrane commonly used in developing solid polymer fuel cell technology.

An important problem in the synthesis of such phosphonates is the limited commercial availability of phosphonic acids with suitable functional groups. It is, therefore, necessary to prepare phosphonic acids as the first step in the preparation of a new proton-conducting phosphonate. In this paper, we report synthesis and characterisation of (i) the new diphosphonic acid *N*,*N*-(diphosphonomethyl)glycine (such a compound offers the prospect of chiral phosphonates, *e.g.* for use as chiral stationary phases in chromatography); and (ii) the Ti^{IV} salt of the new acid. This acidic material is a porous proton conductor.

Experimental

Synthesis

***N*,*N*-(Diphosphonomethyl)glycine, 1.** Phosphorus trichloride (13.1 cm^3, BDH Laboratory Reagent) was added dropwise to a stirred, ice-cold solution of phosphorous acid (12.3 g, Fluka) in 25 cm^3 of deionized water. To this was added a solution containing a stoichiometric equivalent of glycine (Aldrich). The resulting solution was heated to 90 °C and maintained at this temperature during slow addition of paraformaldehyde (9.9 g, Fisons) over a period of 3 h. The resultant solution was then heated at reflux for 1 h, after which the volume of solution was reduced by a factor of 3 by vacuum distillation and an equal volume of ethanol was then added. After crystallisation for 1 day the product was removed by filtration and washed with ethanol prior to drying/storage over saturated NaCl(aq) (relative humidity, RH = 75%).

Elemental microanalysis results obtained for **1** are in excellent agreement with the formulation $(HOOCCH_2)N(CH_2PO_3H_2)_2$ (calc. C, 18.25; H, 4.22; N, 5.32; P, 23.55%; obs. C, 18.22; H, 4.12; N, 5.51; P, 23.47%); thermogravimetry showed no evidence of hydration. Mass spectrometry showed the molecular ion at $m/z = 265$, and intense peaks at $m/z = 81$ (PO_3H_2) and 96 ($CH_2PO_3H_2$), fully consistent with the molecular formula.

Titanium(IV) derivative of *N*,*N*-(diphosphonomethyl)glycine, Ti(dpmg) 2. The synthesis of phosphonates of tetravalent metals shows kinetic control.[7,8] The precipitation of phosphonates usually occurs immediately, generating very small particles. This suggests a high nucleation rate and high insolubility. The use of diphosphonic acids further increases the rate of precipitation, yielding materials of very low crystallinity.

The synthetic method used a reaction mixture containing Ti^{III} which was oxidised slowly to Ti^{IV} by contact with air (this method has been used in the synthesis of crystalline titanium phosphonates with other phosphonic acids).[11,23] *N*,*N*-(Diphosphonomethyl)glycine (**1**, 1 g) was dissolved in 75 cm^3 of deionized water. The solution was mixed with an aqueous solution of $TiCl_3$ (2.3 mol dm^{-3} in 20 mass% HCl, 0.8 cm^3, Aldrich) using a phosphorus to titanium ratio of 4 (phosphonic acid in excess of the stoichiometric requirement). The white solid precipitate formed immediately was heated in contact with the mother liquor for 10 days at 90 °C under reflux conditions, and then recovered by filtration and washed thoroughly with deionized water.

Instrumental

Samples were characterised by thermogravimetry (TG) and differential thermal analysis (DTA) in the range 25–900 °C (heating rate 10 °C min^{-1}) in air using a Stanton Redcroft STA 781 instrument. Elemental microanalysis (C, H, N) used a Perkin-Elmer 240 elemental analyser. IR spectra were recorded as KBr disks on a Nicolet Magna 550 FTIR spectrometer. ^{1}H and ^{31}P solution-state NMR spectra (D_2O solvent) were obtained on a Bruker DRX 400 spectrometer. X-Ray powder diffraction (Philips PW 1050 instrument, modified for computer-driven step-scanning and data acquisition; Ni filtered Cu-Kα radiation, $\lambda = 1.54178$ Å) revealed Ti(dpmg) **2**

to be amorphous to X-rays. Proton-decoupled ^{31}P MAS NMR spectra of solids were recorded on a Varian Unity 300 instrument at a frequency of 121 MHz and employing cross-polarisation with flip-back; chemical shifts are reported with respect to analytical grade 85% H_3PO_4. Solid samples were spun at 2.5 kHz and 3.5 kHz to identify spinning satellites. N_2 adsorption–desorption isotherms were measured volumetrically at 77 K using a Micromeritics Gemini 2375 instrument equipped with a computer-controlled measurement system.

Electrical impedance measurements utilised a Hewlett Packard 4192A LF impedance analyser programmed *via* an IBM-compatible computer for data collection and analysis (using a program embedding EQUIVCRT modelling software[24]). Impedance spectra were recorded at 10 °C intervals in the range $20 \leqslant T/°C \leqslant 90$, using frequencies of 5 Hz to 13 MHz and an oscillating voltage of 300 mV. Pellets (13 mm diameter, 0.7–1.2 mm thickness) were prepared by pressing *ca.* 200 mg of material at 40 kN cm^{-2} in a pellet die. The two flat surfaces were painted with conductive silver paint (Electrodag 915, Acheson Colloids) to give blocking electrodes. The pellet was placed between two copper foils and the sample was spring-loaded to ensure good electrode–electrolyte contact. This assembly was placed inside a cell and maintained at controlled relative humidity [RH: 0% above anhydrous $CaCl_2$, 100% above H_2O(l)]. Prior to measurements, the cell was equilibrated for 1 h at each temperature (this time being found by experience to be twice the minimum necessary for temporal stability in impedance spectra). Experiments were repeated at least three times to ensure reproducible conductivity values and averages are given.

Results and Discussion

Spectra

Fig. 1 shows the IR spectra of *N*,*N*-di(phosphonomethyl)glycine **1** and its Ti^{IV} derivative, Ti(dpmg) **2**. The spectra are seen to have similarities: a strong signal due to the C=O stretching vibration of the carbonyl group of COOH at 1733 cm^{-1} (as in α-amino acids), a doublet in the region 1230–1030 cm^{-1} due to the C—N stretching vibration of the tertiary amine (signals for protonated amine are not detected), a medium intensity signal due to the CH_2 deformation mode of the PCH_2 group at 1421 cm^{-1} and bands at 3000–2800 and 1400–1300 cm^{-1} arising from C—H stretching and deformation modes respectively. In addition to these bands, the spectrum of **1** exhibits a very strong doublet due to the stretching vibration of P=O (hydrogen bonded) at 1244–1150 cm^{-1} and a broad, medium intensity band at 933 cm^{-1} arising from the P—O stretching vibration. The phosphonate Ti(dpmg) **2** shows features typical of such materials: a broad band located at 3500 cm^{-1} associated with the OH bond vibration of interlayer water, a very intense band centred at 1050 cm^{-1} and another at 1615 cm^{-1}, the latter two associated with the P—O bond.[25]

The structure of **1** in solution was confirmed by NMR spectroscopy: δ_H (400 MHz, D_2O): 3.5 (4 H, s, $NCH_2PO_3H_2$), 4.0 (2 H, s, NCH_2COOH) ($COOH$ and PO_3H_2 are not observable owing to chemical exchange); δ_P (161 MHz, D_2O): 9.1 (one phosphorus environment in solution). The ^{31}P MAS NMR spectrum of solid **1** (Fig. 2) showed two peaks (δ_P 13.6, 15.5) with equal intensities (taking account of spinning sidebands). Two phosphorus environments in the solid-state structure might be explained in terms of intramolecular condensation (Scheme 1). The observed peaks correspond, however, to similar chemical shifts and are therefore likely to arise from crystallographically inequivalent phosphonic acid groups. The absence of condensation is consistent with elemental analysis (see earlier).

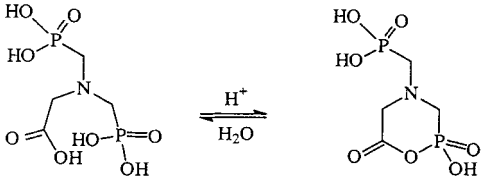

Scheme 1

The possibility of Ti–O–Ti-type aggregates in **2** was examined by calcination (6 h at 900 °C in air); the X-ray diffraction profile for the resulting solid corresponded to that of titanium(IV) pyrophosphate, with no evidence for any form of titanium oxide. Compound **2**, therefore, results from reactions between the diphosphonic acid and the tetravalent metal, with no side reactions resulting in the generation of impurity phases.

Fig. 3 shows the ^{31}P MAS NMR spectrum of Ti(dpmg) **2**. A single broad feature with a shoulder was observed, which can be resolved into two peaks (δ_P 8.9, −1.2) and their spinning sidebands. These peaks do not correspond to signals typical of layered titanium(IV) phosphate (TiP) phases (α-TiP, δ −18.4; γ-TiP, δ −10.9, −32.8; titanium(IV) dihydroxyphosphate, δ

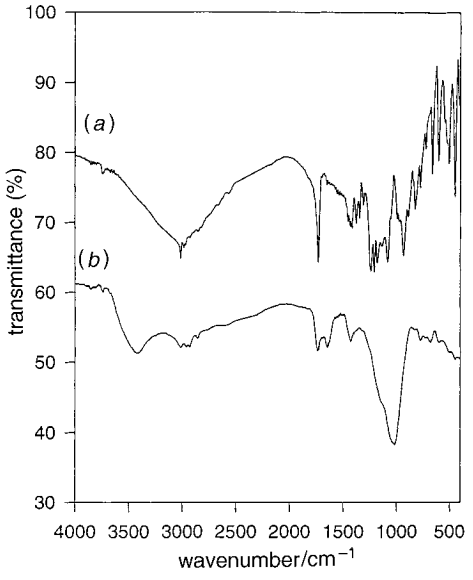

Fig. 1 FTIR spectra of (*a*) *N*,*N*-(diphosphonomethyl)glycine **1** and (*b*) Ti(dpmg) **2**

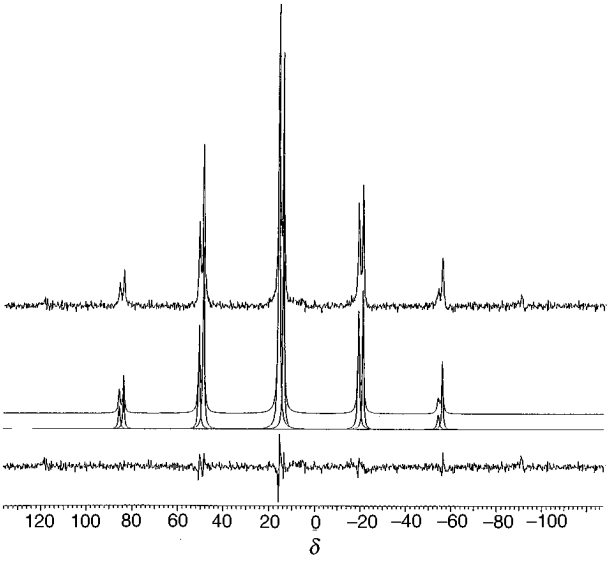

Fig. 2 ^{31}P MAS NMR spectra for *N*,*N*-(diphosphonomethyl)glycine **1**, presented as (top-to-bottom) experimental spectrum, fitted spectrum, Gaussian components and difference plot

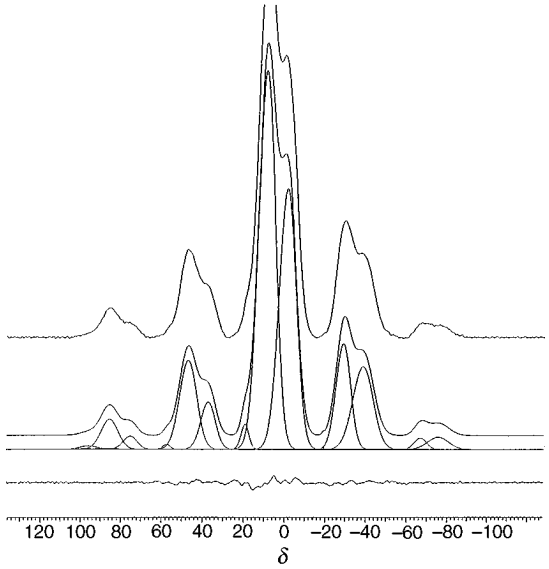

Fig. 3 ^{31}P MAS NMR spectra for Ti(dpmg) **2**, presented as (top-to-bottom) experimental spectrum, fitted spectrum, Gaussian components and difference plot

−6.4).[25] The solid does not contain significant aggregations of titanium phosphate (hydrolysis of **1** would yield phosphoric acid in solution; the degree of hydrolysis at the working pH is shown to be negligible). The synthesis used an excess of diphosphonic acid (see earlier) and, owing to the fast reaction rate, the Ti^{IV} reacts predominantly with only one of the phosphonic acid groups of diphosphonic acid. This is in good agreement with two peaks in the ^{31}P spectrum; a high-field signal for the 'free' phosphonic acid group (δ_P −1.2), and a low-field signal (δ_P 8.9) for the phosphonate group bonded to Ti^{IV}. The peak assigned to the phosphonate site is, however, more intense than that assigned to the phosphonic acid site (integral ratio 1.4 : 1.0, including sidebands), which points to a small fraction of diphosphonate bridging.

Thermal properties

Thermal analyses of Ti(dpmg) **2** showed the water content to depend on the drying and storage conditions. Fig. 4 shows the equilibrated water content as a function of relative humidity (RH) for a sample pre-dried at 50 °C for 2 days.

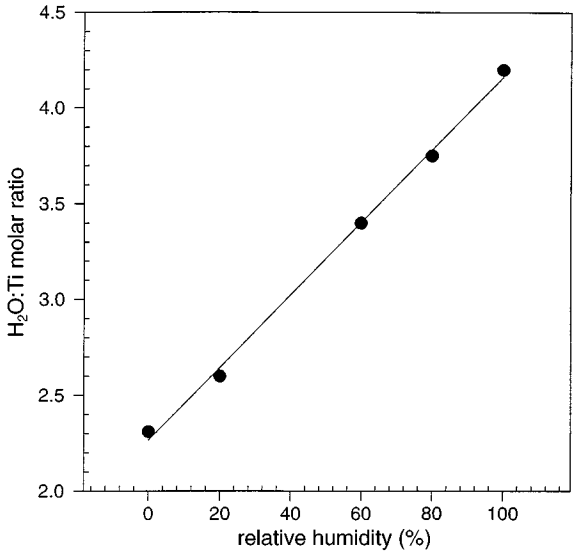

Fig. 4 Equilibrium water content at 25 °C of as-prepared Ti(dpmg) **2** as a function of relative humidity (RH) (analytical chemical formulation as presented in the text refers to material dried at 50 °C)

Fig. 5 shows TG and DTA traces for a sample dried at 50 °C for 2 days and stored over anhydrous $CaCl_2$. The TG trace shows no mass change between 20 and 80 °C, indicating the absence of adsorbed water. The endotherm in the DTA trace at 80–160 °C is assigned to dehydration. The TG trace in the range 80–650 °C indicates a complex dehydration and decomposition sequence (several processes overlap), including the loss of interlayer water, oxidation of the organic portion and condensation of phosphoric groups. The DTA trace shows two exothermic process, assigned as arising from the oxidation of the organic moiety and the phosphate-to-pyrophosphate transformation. The 'free' (non-layer) phosphonic acid groups are transformed in air to water, carbon dioxide and phosphorus pentoxide. The final mass loss takes place at 750 °C and is marked by a sharp peak in the DTA trace, corresponding to a final transformation to cubic pyrophosphate.[26]

On the basis of the total mass loss occurring up to 900 °C (final product TiP_2O_7) and elemental microanalysis, Ti(dpmg) **2** (dried at 50 °C for 2 days, stored over anhydrous $CaCl_2$) can be formulated as

$$Ti[HO_2CCH_2N(CH_2PO_3)_2]_{0.28}[HO_2CCH_2N(CH_2PO_3H_2)CH_2PO_3]_{1.43}\cdot 0.6H_2O$$

[calc. C, 16.27; H, 3.17; N, 4.74%; obs. C, 16.05; H, 3.32; N, 5.11%; TG loss (calc.) = 55.1, TG loss (obs.) = 54.2%]. The ratio of P(phosphonate) : P(phosphonic acid) in this formulation is 1.39 : 1, in good agreement with the NMR result of the previous section.

Porosity

The nitrogen adsorption–desorption isotherm of Ti(dpmg) **2** at 77 K (Fig. 6) corresponds to type IV of the BDDT classification,[27] the form usually associated with titanium(IV) phosphonates.[28] The material has a BET specific surface area of 119 m^2 g^{-1}, a value ten times greater than that typical of layered phosphates. The isotherm has a narrow hysteresis loop of the H3 type, characteristic of aggregates of plate-like particles giving rise to slit-shaped pores.[29]

Fig. 7 shows the cumulative and differential pore volume curves for Ti(dpmg). In the analysis of the desorption isotherm at a relative pressure of *ca.* 0.42 a strong N_2 desorption is observed which gives rise to a peak in the pore radius distribution. The presence of such a peak in a porosity distribution has been considered by the IUPAC Commission,[30] who consider that this effect, typical of many materials, is illusory.[29] The analysis of the desorption isotherm by the slit-shape model

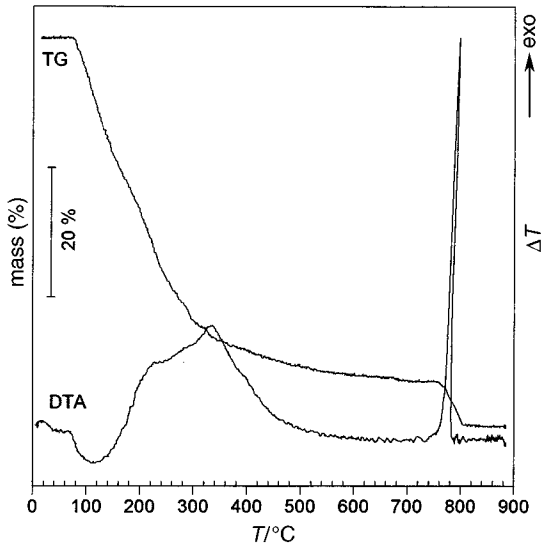

Fig. 5 TG and DTA traces for Ti(dpmg) **2** dried at 50 °C and stored over $CaCl_2$(s)

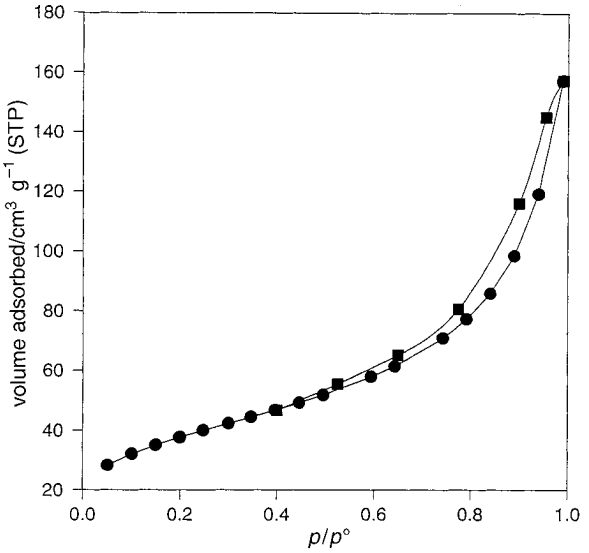

Fig. 6 N_2 adsorption–desorption isotherm at 77 K for Ti(dpmg) **2** degassed at 100 °C

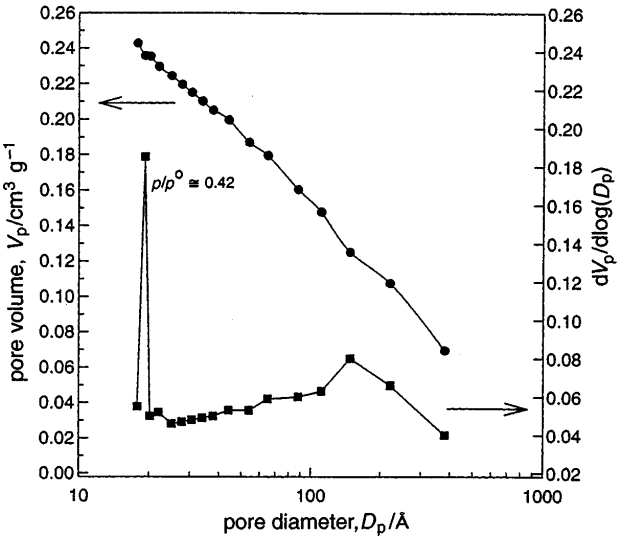

Fig. 7 Cumulative and differential pore volume curves for Ti(dpmg) **2**

gives a porosity distribution with a maximum at 160 Å (D_p is the distance between slit walls).

Impedance spectra and proton conductivity

Characterisation of the electrical conductivity of the phosphonate **2** was carried out by ac impedance measurements. In all cases, the impedance plane plots obtained consisted of a single depressed semicircle (due to the bulk electrolyte resistance) with a low-frequency tail (due to electrode–pellet interfacial impedance); an example is shown in Fig. 8. Such impedance spectra are typical of studies of solid electrolytes with electrodes blocking the ionic charge carriers. The sample resistance was calculated by extrapolation of the high-frequency arc to the real axis. Application of a dc voltage to the sample cell led to very rapid exponential decay in the consequent dc current, this behaviour also being fully consistent with ionic, rather than electronic, conduction in Ti(dpmg).

In the temperature range 20–90 °C the plots $\log_{10}(\sigma T)$ *vs.* $1/T$ are linear and can be modelled with an Arrhenius-type equation $[\sigma T = A \exp(E_a/RT)]$. The Arrhenius plots for **2** at 0% and 100% RH are shown in Fig. 9. E_a and A values are listed in Table 1; errors in these parameters assume an average relative error of 3% on the pellet resistance (justified by the reproducibility of experimental values). E_a increases with

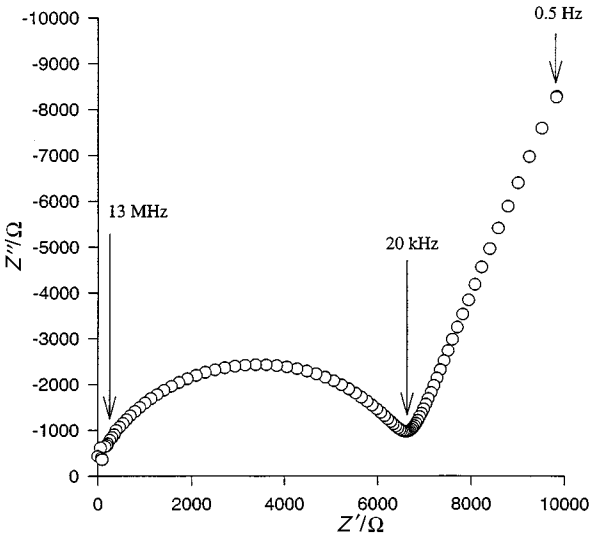

Fig. 8 Impedance spectrum obtained for Ti(dpmg) **2** at 50 °C and RH = 100%

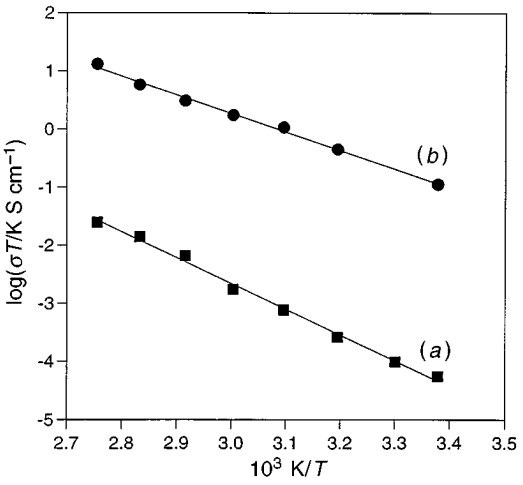

Fig. 9 Temperature dependence of conductivity, σ, for Ti(dpmg) **2** at RH = 0 (*a*) and 100% (*b*)

Table 1 Room-temperature conductivities and Arrhenius parameters for Ti(dpmg) **2** at RH = 0 and 100%

RH (%)	σ/S cm^{-1}	E_a/kJ mol^{-1}	$\log_{10}$ (A/S cm^{-1} K)
0	1.9×10^{-7}	85 (1)	24.5 (0.3)
100	3.7×10^{-4}	63 (2)	22.7 (0.2)

decreasing RH (and level of hydration). At constant temperature, observed values of σ are 2–3 orders of magnitude greater when measurements are carried out at 100% RH atmosphere than those under 0% RH conditions. Water molecules clearly play an important rôle in the conduction process. Conductivity increases by two orders of magnitude temperature is increased [at 0% RH $\sigma(25\,^\circ\text{C}) = 1.9 \times 10^{-7}$ S cm^{-1} and $\sigma(90\,^\circ\text{C}) = 6.9 \times 10^{-5}$ S cm^{-1}; at 100% RH $\sigma(25\,^\circ\text{C}) = 3.7 \times 10^{-4}$ S cm^{-1} and $\sigma(90\,^\circ\text{C}) = 3.5 \times 10^{-2}$ S cm^{-1}].

The strong dependence of conductivity on the water content indicates a vehicular mechanism, where protons are carried by pore water (at low relative humidities loss of water reduces the number of vehicles present and thus conductivity is lower). We could not detect protonic conductivity at $T \geqslant 130\,^\circ$C, and a water-free mechanism involving proton jumps between layer sites or between pendant groups is, therefore, not involved.

The observed conductivities at room temperature are comparable to that of amorphous zirconium phosphate.[31] The

values at elevated temperature are, however, higher than anticipated by that comparison. This increase in conductivity arises from two sources: (1) proton transport in layered phosphates is dominated by surface transport; surfaces areas > 10–$20\ m^2\ g^{-1}$ have not previously been obtained, and only moderate proton conductivities have hitherto been reported at elevated temperatures;[32,33] (2) the phosphonate contains both free carboxylic and free phosphonic acid groups, hence creating a high density of charge carriers for the conduction process.

Conclusions

Ti(dpmg) is a porous proton-conducting material, with conductivity strongly dependent on relative humidity and temperature. At elevated temperature and high relative humidity, conductivities are comparable to that of Nafion under similar conditions [$\sigma(90\ ^\circ C) = 3.5 \times 10^{-2}\ S\ cm^{-1}$ for RH = 100%]. Conductivities are, however, much lower at near-ambient temperatures.

The porosity of Ti(dpmg) rules out its use in an electrolyte separator (*e.g.* in a fuel cell). The strong dependence of σ on relative humidity does, however, point to potential use in a conductimetric humidity sensor.

We thank the Commission of the European Communities for funding (BRITE-Euram II contract BRE2-CT93-0535) and for a personal bursary for E.J. (contract BRE2-CT94-3096). We thank the EPSRC Solid-state NMR Service (Durham) for recording and fitting of MAS NMR spectra.

References

1 S. Drumel, P. Janvier, P. Barboux, M. Bujoli-Doeuff and B. Bujoli, *Inorg. Chem.*, 1995, **34**, 148.
2 D. M. Poojary, Z. Baolong and A. Clearfield, *Angew. Chem.*, 1994, **106**, 2422.
3 S. Bruque, M. A. Aranda, E. R. Losilla, P. Olivera-Pastor and P. Maireles-Torres, *Inorg. Chem.*, 1995, **34**, 893.
4 A. Clearfield and G. D. Smith, *Inorg. Chem.*, 1969, **8**, 431.
5 M. B. Dines, P. Di Giacomo, K. P. Callahan, P. C. Griffith, R. Lane and R. E. Cooksey, in *Chemically Modified Surfaces in Catalysis and Electrocatalysis*, ed. J. S. Miller, ACS Symp. Ser. 192, American Chemical Society, Washington, DC, 1982.
6 G. Alberti, U. Costantino, S. Allulli and N. Tomassini, *J. Inorg. Nucl. Chem.*, 1978, **40**, 1113.
7 K. J. Scott, Y. Zhang, R-C. Wang and A. Clearfield, *Chem. Mater.*, 1995, **7**, 1095.
8 E. Jaimez, A. Bortun, G. Hix, J. R. García, J. Rodríguez and R. C. T. Slade, *J. Chem. Soc., Dalton Trans.*, 1996, 2285.
9 G. L. Rosenthal and J. Caruso, *Inorg. Chem.*, 1992, **31**, 3104.
10 L. Maya and P. O. Danis, *J. Chromatogr.*, 1980, **190**, 145.
11 A. Bortun, A. Clearfield, L. Bortun, E. Jaimez, M. A. Villa-García, J. R. García and J. Rodríguez, *J. Mater. Chem.*, submitted.
12 G. Cao, M. E. García, M. Alcalá, L. F. Burgess and T. E. Mallouk, *J. Am. Chem. Soc.*, 1992, **114**, 7574.
13 M. Ogawa and K. Kurada, *Chem. Rev.*, 1995, **95**, 399.
14 A. Clearfield, in *Surface Organometallic Chemistry: Molecular Approaches to Surface Catalysis*, ed. J. M. Basset, Kluwer Academic Publishers: Norwell MA, 1988; pp. 271–298.
15 M. Casciola, U. Costantino, A. Peraio and T. Rega, *Solid State Ionics*, 1995, **77**, 229.
16 D. A. Burwell and M. E. Thompson, *Chem. Mater.*, 1991, **3**, 91.
17 D. A. Burwell and M. E. Thompson, *Chem. Mater.*, 1991, **3**, 730.
18 C. Bhardwaj, H. Hu and A. Clearfield, *Inorg. Chem.*, 1993, **32**, 4294.
19 C. Y. Ortiz-Avila, C. Bhardwaj and A. Clearfield, *Inorg. Chem.*, 1994, **33**, 2499.
20 K. D. Kreuer, *Chem. Mater.*, 1996, **8**, 610.
21 G. Alberti, M. Casciola, U. Costantino, A. Peraio and R. Vivani, *Solid State Ionics*, 1991, **46**, 53.
22 G. Alberti, M. Casciola, U. Costantino, A. Peraio and E. Monterini, *Solid State Ionics*, 1992, **50**, 315.
23 A. Bortun, E. Jaimez, R. Llavona, J. R. García and J. Rodríguez, *Mater. Res. Bull.*, 1995, **30**, 413.
24 B. A. Boukamp, *Solid State Ionics*, 1986, **20**, 31.
25 B. Bujoli, P. Palvadeau and M. Queignec, *Eur. J. Solid State Inorg. Chem.*, 1992, **29**, 141.
26 K. Segawa, S. Nakata and S. Asaoka, *Mater. Chem. Phys.*, 1987, **17**, 181.
27 S. Brunauer, L. S. Deming, W. S. Deming and E. Teller, *J. Am. Chem. Soc.*, 1940, **62**, 1723.
28 M. A. Villa-García, E. Jaimez, A. Bortun, J. R. García and J. Rodríguez, *J. Porous Mater.*, 1995, **2**, 293.
29 S. J. Gregg and K. S. W. Sing, *Adsorption Surface Area and Porosity*, Academic Press, London, 1982.
30 K. S. W. Sing, D. H. Everett, R. A. W. Haul, L. Moscou, R. A. Pierotti, J. Rouquerol and T. Simieniewska, *Pure Appl. Chem.*, 1985, **57**, 603.
31 G. Alberti and M. Casciola, in *Proton Conductors: Solids, membranes and gels—materials and devices*, ed. Ph. Colomban, Cambridge University Press, Cambridge, 1992, p. 238.
32 R. C. T. Slade and J. A. Knowles, *Solid State Ionics*, 1991, **46**, 45.
33 R. C. T. Slade, H. Jinku and J. A. Knowles, *Solid State Ionics*, 1992, **50**, 287.

Paper 6/06024B; *Received* 2*nd September*, 1996